AGU PUBLICATIONS

Water Resources Research

RESEARCH ARTICLE
10.1002/2013WR014741

An equivalent cross-sectional basis for semidistributed hydrological modeling

Urooj Khan[1,2], Narendra Kumar Tuteja[2], Hoori Ajami[1], and Ashish Sharma[1]

[1]School of Civil and Environmental Engineering, University of New South Wales, Sydney, NSW, Australia, [2]Environment and Research Division, Bureau of Meteorology, Canberra, ACT, Australia

Key Points:
- An approach to reduce the computational time in distributed hydrological model
- Validation is done against observed soil moisture data
- Soil moisture model is based on a 2-D solution of the Richards' equation

Supporting Information:
- Readme
- Table

Correspondence to:
A. Sharma,
A.Sharma@unsw.edu.au

Citation:
Khan, U., N. K. Tuteja, H. Ajami, and A. Sharma (2014), An equivalent cross-sectional basis for semidistributed hydrological modeling, *Water Resour. Res.*, *50*, doi:10.1002/2013WR014741.

Received 12 SEP 2013
Accepted 1 MAY 2014
Accepted article online 6 May 2014

Abstract The computational effort associated with physically based distributed hydrological models is one of their major limitations that restrict their application in soil moisture and land surface flux simulation problems for large catchments. In this work, a new approach for reducing the computational effort associated with such models is investigated. This approach involves the formation of equivalent cross sections, designed in a manner that ensures comparable accuracy in simulating the hydrological fluxes as a fully distributed simulation. Single or multiple equivalent cross sections are formulated in each Strahler's first-order subbasin on the basis of topographic and physiographic variables representing the entire or part of the subbasin. An unsaturated soil moisture movement model based on a two-dimensional solution of the Richards' equation is used for simulating the soil moisture and hydrologic fluxes. The equivalent cross-section approach and the model are validated against observed soil moisture data in a semiarid catchment and found consistent. The results indicate that the equivalent cross-section approach is an efficient alternative for reducing the computational time of distributed hydrological modeling while maintaining reasonable accuracy in simulating hydrologic fluxes, in particular dominant fluxes such as transpiration and soil evaporation in semiarid catchments.

1. Introduction

Physically based distributed hydrological models are valuable tools to simulate spatially distributed information of water balance components including runoff, plant transpiration, soil evaporation, soil moisture, saturated surface area, and deep drainage at every grid cell across the catchment [*Abbott et al*., 1986a, 1986b; *Wigmosta et al*., 1994; *Yang et al*., 1998; *Fortin et al*., 2001a, 2001b]. Although applications of distributed hydrological models have increased due to advances in geographical information systems, remote sensing, and availability of high-resolution spatially distributed data [*Singh and Woolhiser*, 2002; *Wagner et al*., 2009], these models have been criticized for their high computational time, overparameterization, and issues related to the scale of governing equations such as the Richards' equation when it is applied at large catchment scales [*Beven and Binley*, 1992; *Grayson et al*., 1992a, 1992b; *Beven*, 2001; *Singh and Woolhiser*, 2002; *Beven*, 2006; *Kirchner*, 2006; *Beven*, 2012]. Richards' equation is originally derived to simulate fluxes at a point scale. To use the Richards' equation at a large scale, either point scale simulated fluxes are scaled up for a large area or the effective values of soil hydraulic properties are obtained during calibration [*Beven and Binley*, 1992; *Grayson et al*., 1992a, 1992b; *Singh and Woolhiser*, 2002; *Beven*, 2006; *Kirchner*, 2006]. Despite the limitations of Richards' equation for large scale applications and capturing the nonlinearity of hydrological processes at different scales [*Beven and Binley*, 1992; *Beven*, 2001; *Kirchner*, 2006], majority of physically based distributed hydrological models use the Richards' equation (1-D, 2-D, or 3-D) to calculate fluxes in unsaturated zone. These models include MIKE-SHE [*Abbott et al*., 1986a, 1986b], HYDRUS-1D, 2D, and 3D [*Simunek et al*., 1999, 2005, 2006], CATHY [*Paniconi et al*., 2003], GSSHA [*Downer and Ogden*, 2004], MODHMS [*Panday and Huyakorn*, 2004], tRIBS+VEGGIE [*Ivanov et al*., 2008a, 2008b], ParFlow [*Kollet and Maxwell*, 2006], HydroGeosphere [*Brunner and Simmons*, 2012], etc. The implementations of these models for soil moisture and runoff predictions at the catchment scale have been successful even though their high computational time remains a challenge.

Grid size and number of computational grid elements control the computational time as well as the accuracy of simulated hydrological fluxes in distributed hydrologic models [*Bathurst*, 1986]. In the last two decades, various approaches have been introduced to reduce the computational time of distributed

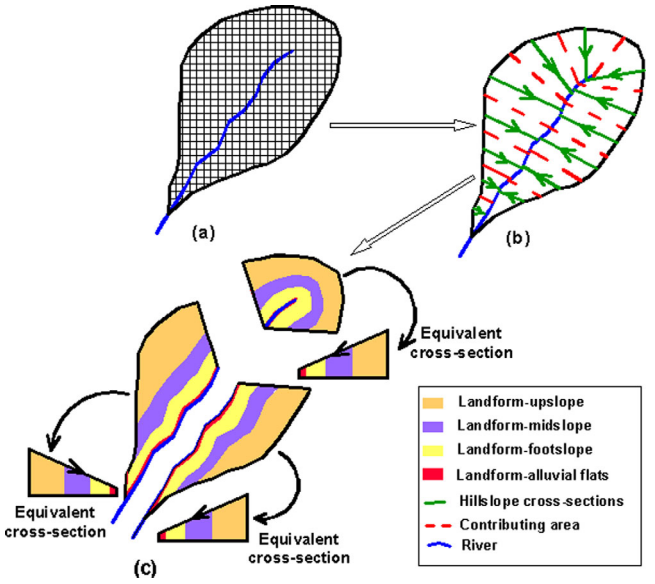

Figure 1. Schematic of equivalent cross-section approach. (a) General concept of 3-D hydrologic modeling in which a first-order subbasin is divided into grids. (b) First-order subbasin is divided into equally spaced multiple hillslope cross sections for 2-D hydrological modeling. (c) First-order subbasin is divided into three equivalent cross sections (right bank, left bank, and head water) for 2-D hydrologic modeling.

hydrological models, mostly involving disaggregating the modeling spatial domain into fewer spatial units in a way that minimizes errors in the simulated hydrologic fluxes [*Beven and Kirkby*, 1979; *Wood et al*., 1988; *Vertessy et al*., 1993; *Flugel*, 1995; *Reggiani et al*., 1998, 1999; *Watson et al*., 1999; *Reggiani et al*., 2000; *Tague and Band*, 2001, 2004; *Reggiani and Rientjes*, 2005; *Summerell et al*., 2005; *Argent et al*., 2007]. *Flugel* [1995] and *Argent et al*. [2007] disaggregated the catchment into Hydrologic Response Units (HRUs) and Functional Units (FUs), respectively, on the basis of homogeneity in topographic and physiographic features of the catchment. *Wood et al*. [1988] used topography, soil, and rainfall patterns to disaggregate the catchment into Representative Elementary Areas (REAs). Later, *Reggiani et al*. [1998, 1999, 2000, 2005] defined Representative Elementary Watersheds (REWs) by dividing the catchment into the first or higher Horton/Strahler stream order subbasins in which the microscale conservation equations are mapped onto the megascale. *Summerell et al*. [2005] divided the entire catchment in four major landforms on the basis of the UPNESS index, which was defined as the ratio of accumulation of upslope area at any given point to its total area. Although disaggregation of a catchment into homogenous computational units was noted to reduce the computational time and units, the contiguity and topological connectivity were not preserved in some of the alternative approaches such as HRUs by *Flugel* [1995], FUs by *Argent et al*. [2007], and four landforms by *Summerell et al*. [2005]. Lack of topological connectivity limits transfer of fluxes from the upper part of a hillslope to lower regions and, hence, is an important attribute to maintain to simulate fluxes with accuracy.

Khan et al. [2013] presented an alternative approach for aggregating spatial information to reduce computational time in distributed hydrologic modeling using fewer computational units than existing methods. They divided an entire catchment into four contiguous major landforms on the basis of variation in topographic and geomorphologic descriptors. In this approach, each hillslope was divided into multiple contiguous landforms to transfer fluxes from the upper part of a hillslope to the lower regions. These landforms constitute the basis for development of the equivalent cross-section approach for semidistributed hydrologic modeling in this paper (Figures 1a–1c). The term "equivalent cross section" here and remainder of the paper refers to a cross section which is representative of a section or an entire area of a first-order subbasin. In the equivalent cross-section approach, a hillslope is divided into approximately uniformly spaced multiple hillslope cross sections along the catchment boundary of first-order subbasin (Figure 1b). A single or multiple equivalent cross sections are formulated using appropriate weighting of topographic and physiographic features of a section or an entire first-order subbasin on a landform basis (Figure 1c), described in detail in section 4. The number of equivalent cross sections in a subbasin depends on the soil-type pattern within the subbasin. The concept of equivalent cross-section approach is different from the earlier approaches developed to disaggregate the catchment into smaller spatial units, i.e., HRUs by *Flugel* [1995], FUs by *Argent et al*. [2007], REAs by *Wood et al*. [1988], and hillslope patches by *Tague and Band* [2001]. In the majority of previous approaches, catchments were divided into smaller spatial units on the basis of similarity in topographical and physiographical features, whereas in the equivalent cross-section approach, a representative/equivalent cross section is formulated to represent a section or an entire area of a first-order subbasin. The proposed equivalent cross-section approach reduces the computational time of hydrologic

modeling significantly, while maintaining almost the same order of accuracy in the estimated hydrological fluxes, in particular transpiration and soil evaporation, as these are the dominant fluxes in the semiarid catchments considered in this study. Further, the equivalent cross-section approach also maintains the topological connectivity between spatial units for transferring of the hydrological fluxes from the upper part of the subbasin to the lower part.

The rest of the paper is organized as follows. We next present details about the study region the approach is illustrated over, followed by a summary of the soil moisture modeling scheme and presentation of the equivalent cross-section approach. Selected results have been presented articulating the exact form of the approach that is recommended. Next, results from the use of the equivalent cross sections are discussed, and validated against in situ soil moisture observations. Key conclusions from the study are presented next.

2. Study Sites

The study area includes the McLaughlin catchment with the area of 459 km^2. The McLaughlin catchment is a subcatchment of the Snowy River located in the Snowy Monaro region in south-eastern New South Wales (NSW), Australia (Figure 2). *Teng et al*. [2008] delineated four climate zones (A: $<$600 mm/yr, B: 600–750 mm/yr, C: 750–900 mm/yr, and D: $>$900 mm/yr) for the Snowy Monaro region based on climate surfaces of the Australian continent [*Jeffrey et al*., 2001]. The mean annual rainfall and pan evaporation for the McLaughlin catchment are 650 mm/yr and 1425 mm/yr, respectively. The McLaughlin and its neighboring catchments have been under hydrologic investigation for the last 10 years due to the changes in land use during the last 50 years [*Tuteja et al*., 2007].

Khan et al. [2013] divided the entire McLaughlin catchment into four contiguous major landforms on the basis of variation in topographic, physiographic, and geomorphologic descriptors, which includes Cumulative Area Distribution (CAD) curve, slope, curvature, Compound Topographic Index (CTI), and Multiresolution Valley Bottom Flatness Index (MRVBF) using a 25 m Digital Elevation Model (DEM). The DEM data are derived from contour and drainage data of NSW topographic maps and were provided by the former Department of Environment, Climate Change and Water, NSW. Delineated landforms are named landform-upslope, midslope, footslope, and alluvial flats on the basis of the distances of these landforms from the center of the river (0–25, 25–75, 75–350, and greater than 350 m) [*Khan et al*., 2013]. These thresholds were based on similarity in topographic, physiographic, and geomorphologic descriptors of the catchment. Seven Strahler's first-order subbasins of McLaughlin catchment located in different rock types and altitudes are considered in this study (Figure 2). All major landforms of the McLaughlin catchment are available in these subbasins.

The Wagga-Wagga experimental catchment is located at approximately 5 km south-west of Wagga-Wagga, at the New South Wales Office of Environment and Heritage (Figure 2). Observational data from this highly instrumented catchment are used for validation of (1) the two-dimensional soil water balance model [*Tuteja et al*., 2004] used in this study and (2) the equivalent cross-section approach. The mean annual rainfall and pan evaporation on the basis of 1997–1999 data for the Wagga-Wagga experimental catchment are 534 and 1357 mm/yr, respectively. The elevation and distance information on multiple hillslope cross sections in the Wagga-Wagga experimental catchment are obtained from a contour map of 2.5 m interval [*Tuteja et al*., 2000]. The Wagga-Wagga experimental catchment is a small catchment with no DEM data; therefore, it was not possible to implement the landform delineation methodology of *Khan et al*. [2013] for this catchment and, hence, each individual soil type is considered as a landform. Landforms upslope, midslope, and footslope closely relate to soil types: Tenosols, Chromosols, and Sodosols, respectively (Figure 2) [*Isbell*, 1996]. The fourth landform (alluvial flats) is not present in this catchment. The catchment areas and attributes of seven first-order subbasins in McLaughlin catchment and Wagga-Wagga experimental catchment are presented in Table 1.

2.1. Land Use

The subcatchments of Snowy Monaro region were divided into five land use categories, i.e., crop, native woody (forest), pines, pasture, and improved pasture by *Tuteja et al*. [2006] (Table 1). The land use type of Wagga-Wagga experimental catchment is Phalaris perennial grassland. The Leaf Area Index (LAI) and root biomass distributions of seven subbasins in the McLaughlin catchment are taken from *Tuteja et al*. [2006,

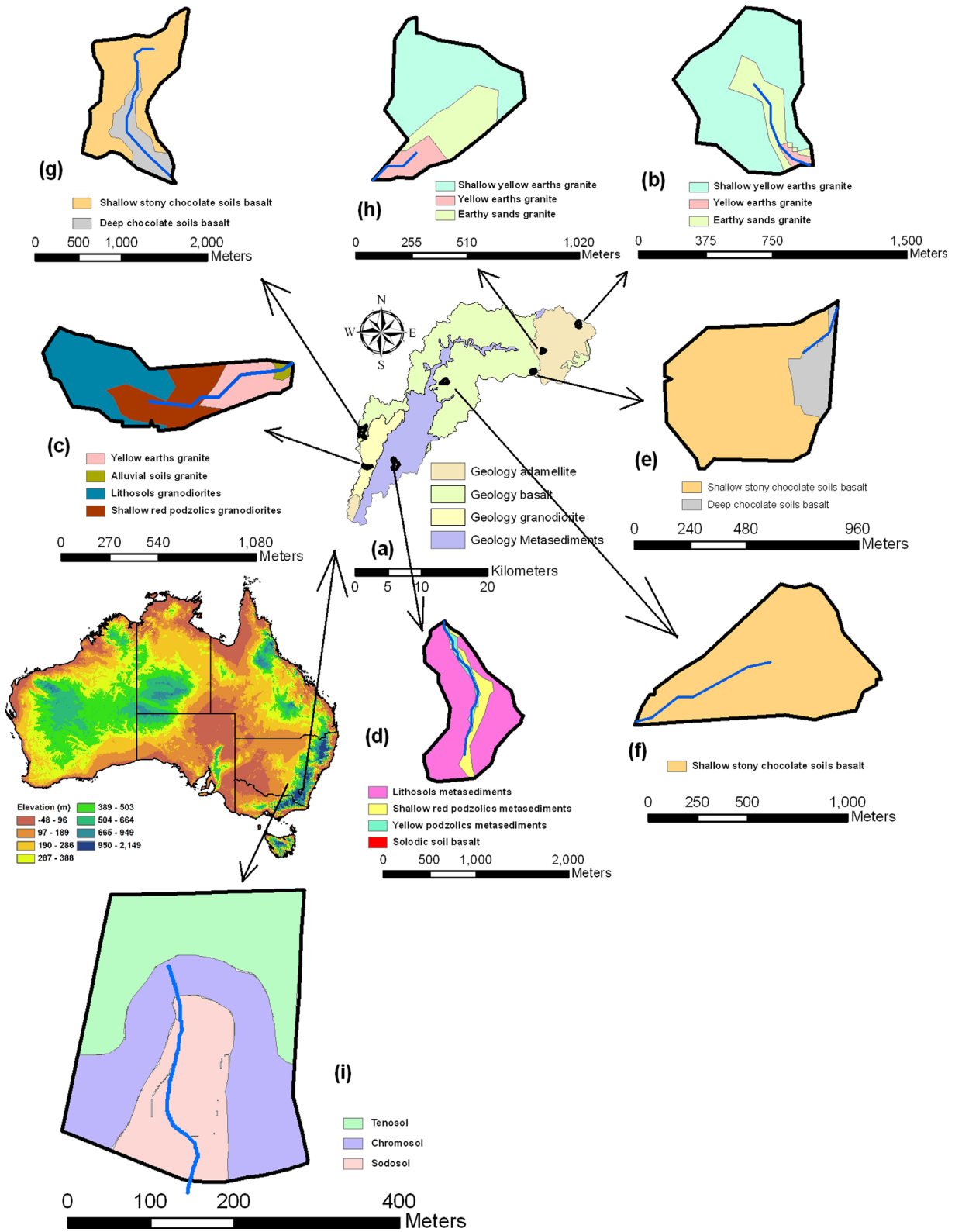

Figure 2. Location of study sites considered in the study. (a) McLaughlin catchment marked with seven first-order sub-basins. (b) M-1, (c) M-2, (d) M-3, (e) M-4, (f) M-5, (g) M-6, (h) M-7, and (i) Wagga-Wagga experimental catchment. The soil-type maps are presented in each sub-basin.

Table 1. Subbasins Properties[a]

Subbasin Number/Name	Catchment	Area (Ha.)	Climate Zone	Land Use Types
M-1	McLaughlin	47.06	C	Native woody (forest)
M-2	McLaughlin	42.69	A	Native woody (forest) and pasture
M-3	McLaughlin	105.36	A	Native woody (forest)
M-4	McLaughlin	38.64	B	Pasture
M-5	McLaughlin	48.77	A	Pasture
M-6	McLaughlin	126.62	B	Pasture
M-7	McLaughlin	28.70	B	Native woody (forest)
Wagga	Wagga-Wagga experimental catchment	8.55		Phalaris grass

[a]The climate zones are defined based on variability of annual rainfall within a certain limit and they were delineated by *Teng et al.* [2008] for the Snowy Monaro region based on climate surfaces of the Australian continent [*Jeffrey et al.*, 2001]. The total annual rainfall for four climate zones are A: <600 mm/yr, B: 600–750 mm/yr, C: 750–900 mm/yr, and D: >900 mm/yr.

2007], which was based on detailed exploratory work and knowledge of plant physiologists at the site [*Tuteja et al.*, 2006, 2007]. The Leaf Area Index (LAI) and root biomass distributions for Wagga-Wagga catchment are taken from *Tuteja et al.* [2000].

2.2. Soil Types

The McLaughlin catchment consists of four major rock types, i.e., Adamellite, Basalt, Granodiorite, and Metasediments (Figure 2a) [*Murphy et al.*, 2005]. Seven subbasins are selected in these four rock types in such a manner that at least one subbasin is taken from each rock type as the soil hydraulic properties vary significantly if it is formed on different rock type (Figures 2a–2h). These subbasins also spread across the high and low elevation areas and cover various land use and climate zones (Table 1). A soils information package was developed by *Murphy et al.* [2005], comprising spatial distribution of soils, soil depth, and soil hydraulic properties for the McLaughlin catchment on the basis of their respective parent material, ancillary data sources, and field observations (Figures 2b–2h). Individual soil types at a 25 m resolution were formulated by *Murphy et al.* [2005] using metadata associated with each type (e.g., particle size analysis and bulk density). This metadata were used with Pedotransfer Function (PTF) models of *Minasny and McBratney* [2002] and *Schaap and Leij* [1998] to determine the soil hydraulic properties (see table in the supporting information). These soil hydraulic properties are used in this study without any adjustment. *Murphy et al.* [2005] determined the soil depths using the methodology of *McKenzie et al.* [2003]. The soil depths are higher near valley bottoms and lower at the top of hillslopes ranging from 0.15 m to 6 m in the McLaughlin catchment.

The Wagga-Wagga experimental catchment consists of three predominant soil types: Haplic Mesotropic Red Chromosol (Chromosol), Eutrophic Mottled-Mesonatric Brown Sodosols (Sodosol), and Palic Paralythic Leptic Tenosol (Tenosol) based on the Australian soil classification system [*Isbell*, 1996] (Figure 2i). The Tenosols occur mainly on the ridge and upper slopes. Chromosols occur at slight break of slope between the ridge and crest, and the midslopes and Sodosols are restricted to the drainage lines [*Tuteja et al.*, 2000]. The soil hydraulic properties of Tenosols, Chromosols, and Sodosols were derived from extensive laboratory and in situ experiments [*Tuteja et al.*, 2000] (see table in the supporting information).

3. Numerical Solution of the Two-Dimensional Richards' Equation

To formulate the equivalent cross-section approach, a 2-D physically based distributed hydrological model referred as Unsaturated Soil Moisture Movement Model (U3M-2D) is used. The model was developed by *Tuteja et al.* [2004] based on an extended two-dimensional version of U3M-1D [*Vaze et al.*, 2004] (see http://www.toolkit.net.au/Tools/CLASS-U3M-1D/publications for details on model equations, section 3.11–3.13). The input data required to run the model are rainfall, pan evaporation, radiation, maximum and minimum temperature, soil hydraulic properties, land use type, depth of each soil type, root biomass distribution, and leaf area index (LAI). U3M-2D performs a local water balance for each pixel of the hillslope cross section along the vertical direction by dividing the entire soil depth into four soil horizons or soil materials. Each soil material is further divided in thin soil layers for computation of vertical water balance. Gravity drainage, capillary rise, evapotranspiration, and horizontal variably

saturated inflow from upslope areas and downslope outflow are computed for each pixel. The U3M-2D model uses Richards' equation in the vertical direction with a variable subdaily time step for partitioning of water balance (transpiration, soil evaporation, deep drainage, and soil moisture excess) in the unsaturated zone. The subdaily computational time step varies from 5 min to 1 h, according to rainfall intensity, 5 min time step is considered for very high intensity rainfall of the order of 1000 mm/d and 1 h for low intensity rainfall of about 5 mm/d. In between these two extremes, the time steps are adaptively adjusted depending on transient soil moisture conditions. Potential plant transpiration and potential soil evaporation are calculated from potential evapotranspiration on the basis of LAI and land use type. The model calculates actual transpiration and soil evaporation dynamically on the basis of available water in the root zone as well as root biomass distribution.

The U3M-2D model uses a specified flux (rainfall minus potential soil evaporation) boundary condition at the soil surface and a free drainage boundary condition at the bottom of the soil profile. Specified head or specified flux boundary condition is also available in the model for the bottom of the soil profile. A specified flux representing soil moisture contribution from upslope areas is used across each soil material of the soil profile. Initial soil moisture conditions for each soil material are specified as a function of residual soil moisture, saturated soil moisture, and degree of specific saturation.

The model uses one-dimensional solution of Richards' equation for performing the local vertical water balance for each pixel on the hillslope cross section. After that, any moisture arising from variably saturated conditions and in excess of the soil moisture holding capacity is pooled over the respective soil material and transferred horizontally to downslope pixel using the unsaturated form of the Darcy's law (introduces lag) (see *Tuteja et al*. [2004, section 3.11–3.13] for details). Simulated fluxes from the model are soil moisture across the profile, actual transpiration, soil evaporation, horizontal fluxes, and drainage below the root zone (deep drainage).

4. Development and Evaluation of the Equivalent Cross-Section Framework

To reduce the computational time/units in distributed hydrological modeling, a new framework of equivalent cross section is developed. The equivalent cross sections are formulated for Strahler's first-order subbasins. These first-order subbasins were delineated by *Khan et al*. [2013] using the TauDEM tool (http://hydrology.uwrl.usu.edu/taudem/taudem5.0/index.html) developed by *Tarboton* [1997]. To formulate the equivalent cross sections, topographical, and physiographical properties for the first-order subbasins are averaged in a systematic manner using the different weighting schemes presented below. The accuracy of the equivalent cross-section approach is assessed against the distributed modeling approach, where a given first-order subbasin is divided into multiple cross sections.

4.1. Distributed Hydrologic Modeling at Multiple Cross Sections Across a Hillslope in a First-Order Sub-Basin

To perform distributed hydrologic modeling on seven subbasins of McLaughlin catchment and Wagga-Wagga experimental catchment, the subbasins are divided into equally spaced multiple cross sections across a hillslope (Figure 1b), and actual topographical and physiographical features of each pixel inside a cross sections are considered for the 2-D distributed modeling. The 2-D distributed hydrologic modeling on each cross section is performed using the U3M-2D model [*Tuteja et al*., 2004]. Note that the distributed modeling term here and in the remainder of the paper refers to the 2-D distributed modeling on each pixel of multiple cross sections. The reason for performing the distributed modeling in this manner is to make an appropriate comparison between the equivalent cross-section-based and the distributed modeling results, as the same 2-D model is used in both cases. If a 3-D model will be used as a means for comparison, some issues regarding the model structure and numerical solution will arise and effects of reducing computational elements cannot be truly evaluated. The dashed center lines are drawn between the two hillslope cross sections in all subbasins, and the area enclosed between the two center lines of a cross section is considered as the contributing area of that cross section (Figure 1b). The number of cross sections, range of cross-sectional lengths, contributing areas, slopes, and soil depths in each subbasin are presented in Table 2. Daily rainfall, pan evaporation, radiation, and maximum and minimum temperature for the period of 1975–2000 are used for hydrologic modeling. Potential evapotranspiration was derived from pan evaporation data and the appropriate pan factor to correct for differences in radiation, temperature, and vapor pressure deficit. Wagga-Wagga experimental catchment has short-term daily climate records for the period of

Table 2. Summary of Cross-Section Properties in Each Subbasin

Subbasin	Number of Cross Sections in the Subbasin	Range of Cross-Sections Length (m)	Range of Cross Sections Contributing Area (Ha)	Range of Cross-Sections Slope	Range of Cross-Sections Soil Depth (m)
M-1	18	125–450	1.04–4.45	0.034–0.264	0.34–6.0
M-2	21	50–650	0.67–5.23	0.046–0.334	0.62–4.73
M-3	22	75–500	1.51–9.70	0.102–0.542	0.42–3.96
M-4	18	50–675	0.17–6.32	0.009–0.121	0.53–6.26
M-5	22	50–550	0.21–4.41	0.031–0.254	0.40–1.13
M-6	20	75–575	1.25–13.13	0.0005–0.121	0.56–6.01
M-7	21	50–625	0.09–2.94	0.029–0.146	0.41–3.02
Wagga	11	140–260	0.38–1.02	0.046–0.153	0.61–2.60

October 1997 to November 1999 which are used in this study. This data include rainfall, potential evaporation, radiation, and maximum and minimum temperature.

In distributed modeling, actual topographic and physiographic properties, i.e., length, slope, elevation, soil depth, soil type, and land use of each pixel in a cross section, are used in the model for simulating soil moisture and hydrological fluxes including horizontal flux, deep drainage, transpiration, and soil evaporation. Note that no averaging or weighting of any topographical and physiographical variables is performed in the distributed modeling described here. Total runoff from every cross section is calculated by summing up the horizontal flux from the last pixel of a cross section and the average deep drainage of all pixels. Simulated hydrological fluxes from each subbasin are presented in two ways. First, simulated hydrologic fluxes from each cross section are multiplied by the respective contributing area to get the volumetric flux of a cross section. Volumetric fluxes from all cross sections in a subbasin are aggregated to obtain the total fluxes of a subbasin, which is referred to as reference fluxes. These reference fluxes are compared with the fluxes from the equivalent cross-section approach later to assess the suitability of the equivalent cross section in simulating hydrologic fluxes relative to the case where multiple cross sections are used, i.e., distributed modeling is performed on a 2-D cross-sectional basis across the first-order basin. The simulated hydrological fluxes from distributed modeling of each cross section in a subbasin are also multiplied by the total area of the subbasin, to examine whether the fluxes of each cross section can be representative of the entire subbasin fluxes. For example, subbasin M-3 contains 22 cross sections (Table 2). The simulated fluxes from each cross section are multiplied by the total area of the subbasin M-3 to generate 22 representative fluxes for the entire subbasin. These fluxes are compared with the reference fluxes to examine whether a single cross section can represent the entire subbasin.

Out of eight subbasins, results of four subbasins are presented (Figures 3a–3d). These four subbasins include M-3, M-5, M-7, and Wagga-Wagga. The subbasin M-3 located in Metasediments rock types is included because the soil type in this basin is consistent with landform pattern, i.e., different soil near the center of the river and changes toward the ridge line (Figure 2d and Table 3). The subbasin M-5 contains only one soil type and located in Basalt rock type (Figure 2f and Table 3). The subbasin M-7 located in Adamellite rock types contains three types of soils with complex patterns that are not consistent with landform pattern or any other systematic pattern (Figure 2h and Table 3). The Wagga-Wagga experimental catchment is used for evaluation of results against observed soil moisture data (Figure 2i and Table 3).

The comparison between reference case and individual cross section for cumulative total runoff shows significant variability. The major cause of this variability is the variation in cross-sectional lengths, slopes, soil depths, and soil types within a subbasin (Table 2). However, fluxes of a few individual cross sections are close to that for the reference case (Figures 3a–3d). This result confirms that not every cross section in a subbasin can represent the hydrologic fluxes of the entire subbasin, and only a few cross sections whose fluxes are close to the reference fluxes are representative of the subbasin. The variability in transpiration and soil evaporation is comparatively less than the cumulative total runoff (results are not shown but available from the authors on request). These results indicate that if a subbasin is to be accurately represented by a single or multiple equivalent cross sections, i.e., runoff is close to the reference runoff, then an intelligent weighting of the cross sections based on topographic and physiographic properties is required.

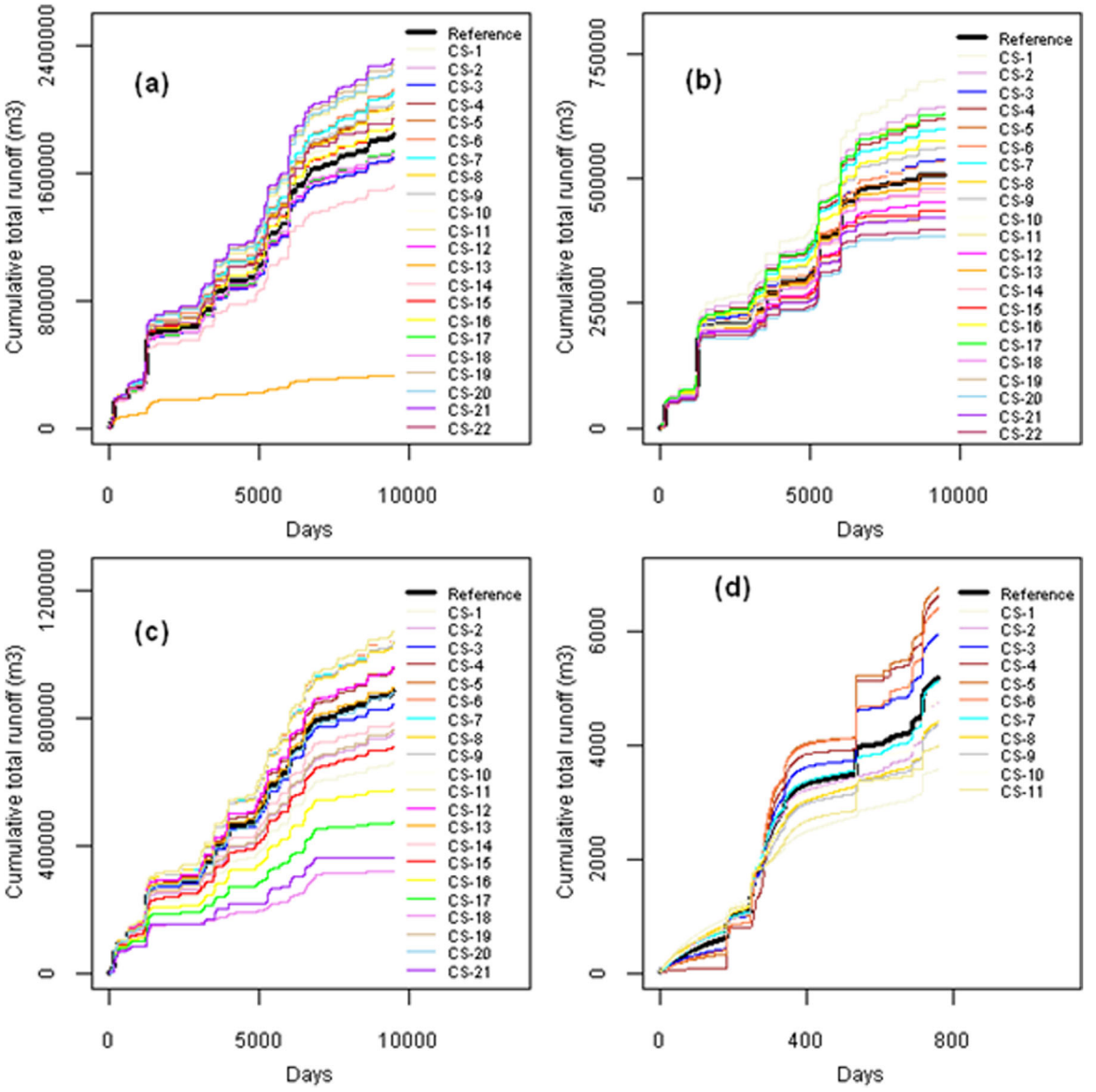

Figure 3. Cumulative total runoff volume for reference case and for each cross section representing the entire subbasin. (a) M-3, (b) M-5, (c) M-7, and (d) Wagga-Wagga. The reference fluxes are calculated by multiplying the contributing area of each cross section with its simulated fluxes and then aggregating of individual volumetric fluxes to obtain total volumetric fluxes of the entire subbasin. The representative fluxes from individual cross sections are calculated by multiplying the total area of a subbasin with the simulated fluxes from each cross section.

4.2. Homogenization Test for Developing Equivalent Cross Sections

To ascertain the key factors that should influence an equivalent cross section, a homogenization test is carried out as described below. Four topographic and physiographic variables, which are the major drivers for generating the fluxes in 2-D distributed hydrologic modeling, are considered in the homogenization test. These variables are cross sectional length, slope, soil depth, and soil types. These four variables are altered in a systematic manner to quantify their impact on simulated fluxes. To conduct the homogenization test, subbasin M-2 and M-7 of McLaughlin catchment are considered because of their complex shapes and soil-type patterns (Figures 2c and 2h). A total of 21 cross sections are drawn in each subbasin to perform the distributed hydrologic modeling at multiple hillslope cross sections (section 4.1). These cross sections being the basis for the homogenization test results presented later.

In the homogenization test, hillslope properties for all cross sections are assumed to be constant, and only the value of one variable in all 21 cross sections is chosen based on actual catchment properties. For example, in homogenization test of a cross sectional length, the length of all 21 cross sections are based on the

Table 3. Description of Soil-Type Pattern

Subbasin Number/Name	Catchment	Rock Types	Soil-Type Pattern	Number of Equivalent Cross Sections Required to Represent a Subbasin
M-1	McLaughlin	Adamellite	Consistent with landform pattern[a]	3 (1 left bank, 1 right bank, and 1 head water)
M-2	McLaughlin	Granodiorite	Complex pattern[b]	3 (one in each soil type)
M-3	McLaughlin	Metasediments	Consistent with landform pattern[a]	3 (1 left bank, 1 right bank, and 1 head water)
M-4	McLaughlin	Basalt	Complex pattern[b]	3 (one in each soil type)
M-5	McLaughlin	Basalt	No pattern[c]	1 (for entire subbasin)
M-6	McLaughlin	Basalt	Consistent with landform pattern[a]	3 (1 left bank, 1 right bank, and 1 head water)
M-7	McLaughlin	Adamellite	Complex pattern[b]	3 (one in each soil type)
Wagga	Wagga-Wagga experimental catchment		Consistent with landform pattern[a]	3 (1 left bank, 1 right bank, and 1 head water)

[a]Consistent with landform pattern, i.e., different soil near the center of the river and changes toward the ridge line.
[b]Complex pattern, i.e., complex soil type with no systematic pattern.
[c]No pattern, i.e., single soil type.

actual lengths, whereas the slope, soil depth, and soil type are constant for all the cross sections (obtained from average values of slope, soil material depth, and dominant soil type for all pixels of all 21 cross sections). When treated in this way, differences between the cross sections are only in the lengths for this case. In a similar way, when the homogenization test of soil type is conducted, the length, slope, and soil depth of all cross sections are assumed to be constant and actual soil type of cross sections are considered. When treated in this way, differences between the cross sections are only in the soil types for this case. All of these cross sections are simulated in a fully distributed manner using the U3M-2D model as mentioned in section 4.1 and reference fluxes are generated.

A single equivalent cross section is formulated based on the four landforms (upslope, midslope, footslope, and alluvial flats) delineated by *Khan et al*. [2013]. Note that whenever the term "equivalent cross section" is used in the paper then the topographic and physiographic variables of a section or an entire subbasin are weighted in a systematic manner on a four landform basis. The length of single equivalent cross section is obtained by arithmetic averaging of length of 21 cross sections using equation (1). The slope and soil depth of each landform in single equivalent cross section are obtained by length-weighted averaging of slope and soil depth of 21 cross sections using equations (2) and (3)

$$\bar{l}_j = \frac{1}{I}\sum_{i=1}^{I} l_{i,j}, \quad j = 1, 2, \ldots\ldots, J \ \text{(landforms)} \tag{1}$$

$$\bar{s}_j = \frac{\sum_{i=1}^{I} s_{i,j} \times l_{i,j}}{\sum_{i=1}^{I} l_{i,j}}, \quad j = 1, 2, \ldots\ldots, J \ \text{(landforms)} \tag{2}$$

$$\bar{d}_{j,k} = \frac{\sum_{i=1}^{I} d_{i,j,k} \times l_{i,j}}{\sum_{i=1}^{I} l_{i,j}}, \quad \begin{matrix} j = 1, 2, \ldots\ldots, J \ \text{(landforms)} \\ k = 1, 2, \ldots\ldots, K \ \text{(soil materials)} \end{matrix} \tag{3}$$

where $i = 1, 2, \ldots\ldots, I$ = number of cross-sections, $j = 1, 2, \ldots\ldots, J$ = number of landforms, $k = 1, 2, \ldots\ldots, K$ = number of soil materials, $l_{i,j}$ = length of landform j of cross section i, $\bar{l}_j$ = average length of landform j across all cross sections I, $s_{i,j}$ = slope of landform j of cross section i, $\bar{s}_j$ = average slope of landform j across all cross sections I, $d_{i,j,k}$ = depth of soil material k of landform j of cross section i, $\bar{d}_{j,k}$ = average depth of soil material k of landform j across all cross sections I.

Before adopting the length-weighted averaging scheme for formulating an equivalent cross section on a four landform basis, different averaging schemes of topographic and physiographic attributes were examined at the catchment or landform scales for subbasins M-1, M-2, and M-3. These averaging schemes included arithmetic averaging, length-weighted averaging, area-weighted averaging at the landform scale, and arithmetic averaging of catchment properties at the catchment scale. None of these approaches were found to consistently perform well for all hydrological fluxes in all the subbasins, but the length-weighted averaging results were better than other schemes in majority of the cases. Considering the logic behind the averaging schemes and based on the results, the length-weighted averaging at the landform scale is

adopted for the equivalent cross-section formulation. In the length-weighted averaging scheme, proper weights are given to the topographic/physiographic variables of a cross section on the basis of cross section's length, whereas in the arithmetic averaging, equal weights would have to be given to the topographic/physiographic variables instead.

The length-weighted averaging is not used for deciding the soil type of an equivalent cross section as the soil hydraulic properties are highly nonlinear in nature. Instead, the dominant soil type in each landform is considered. The dominant soil type is specified by computing percentage area of each soil type within a given landform and identifying the dominant soil type. Subsequently, soil hydraulic properties are assigned to a given landform based on the dominant soil type. Note that an equivalent cross section consists of four landforms. Therefore, separate soil type along with soil hydraulic properties can be provided for each landform to account for variability in soil hydraulic properties in the horizontal direction. To account for variability of soil hydraulic properties in the vertical direction, the soil column along each pixel of the landform is divided into four soil horizons, and hydraulic properties of each horizon of the dominant soil type in a landform is provided in the respective horizon. This single equivalent cross section is simulated using U3M-2D model to generate the fluxes. The generated fluxes are multiplied by the area of the subbasin to get the total fluxes from the subbasin. The fluxes of the single equivalent cross section are compared with the reference fluxes and presented in Figures 4a–4d and 5a–5d for subbasin M-2 and M-7.

This homogenization test quantifies the accuracy lost in averaging individual variables during single equivalent cross section formulation. It is clear from Figures 4a–4d and 5a–5d that the greatest accuracy loss occurs in the case of soil type, whereas little accuracy is lost in length, slope, and soil depth weighting. The homogenization test of single equivalent cross section concludes that (1) if a subbasin contains multiple soil types with complex pattern, then a single equivalent cross section is not sufficient to represent the subbasin (as in the M-2 and M-7 subbasins) and (2) if there is a single soil type across the subbasin then single equivalent cross section can represent entire subbasin. If there is a single soil type in a subbasin, then the homogenizations test based on soil type does not make a difference in simulated fluxes between equivalent cross section and reference flux, leading to the second conclusion drawn above. Because the soil type is the same across the catchment, the homogenization can be only performed based on length, slope, and soil depth in this case. It is already proved from the homogenization test that the loss of accuracy in averaging of length, slopes, and soil depth is negligible. If the accuracy loss due to soil type will also be negligible in subbasins with one single soil type, then a single equivalent cross section will be sufficient to represent this subbasin.

In the next attempt, the homogenization test is carried out to formulate three equivalent cross sections in a subbasin each representing left bank, right bank, and head water catchment. The averaging of topographic and physiographic variables done separately for left bank, right bank, and head water catchment in a similar manner as for the single equivalent cross section, i.e., equations (1)–(3) and dominant soil type of each landform also applied separately to left bank, right bank, and head water. The simulated fluxes from U3M-2D model for each equivalent cross section are multiplied by the respective bank area and then aggregated over a subbasin to obtain total fluxes of the entire subbasin (Figures 4a–4d and 5a–5d). It is clear from Figures 4a–4d and 5a–5d that using three equivalent cross sections improves the accuracy of simulated fluxes compared to a single equivalent cross section. This improvement is consistent for all variables except for soil type.

The results of the homogenization test of single and three equivalent cross sections confirm that the soil type is the most important variable to formulate an equivalent cross section. The formulation of equivalent cross section should be performed in a systematic manner by incorporating variability in the soil type, as it is linked with the variability of soil hydraulic properties which significantly influences the fluxes. Therefore, another attempt is made for formulating the equivalent cross sections such that each soil type has its own equivalent cross section. Subbasin M-2 contains four types of soils and subbasin M-7 contains three types of soils. Only three dominant soil types are considered for formulating the equivalent cross sections for subbasin M-2 because the area covered under alluvial soils granite in subbasin M-2 is negligible (Figures 2c and 2h). Three equivalent cross sections are formulated on each subbasin based on the soil types with each equivalent cross section representing one soil type. The weighted averaging of topographic and physiographic variables for each soil type is done in a similar manner as that of single equivalent cross section (equations (1)–(3) and dominant soil type). The simulated fluxes from the U3M-2D model are multiplied by the aggregated contributing area of all cross sections located in individual soil polygon, and then the fluxes

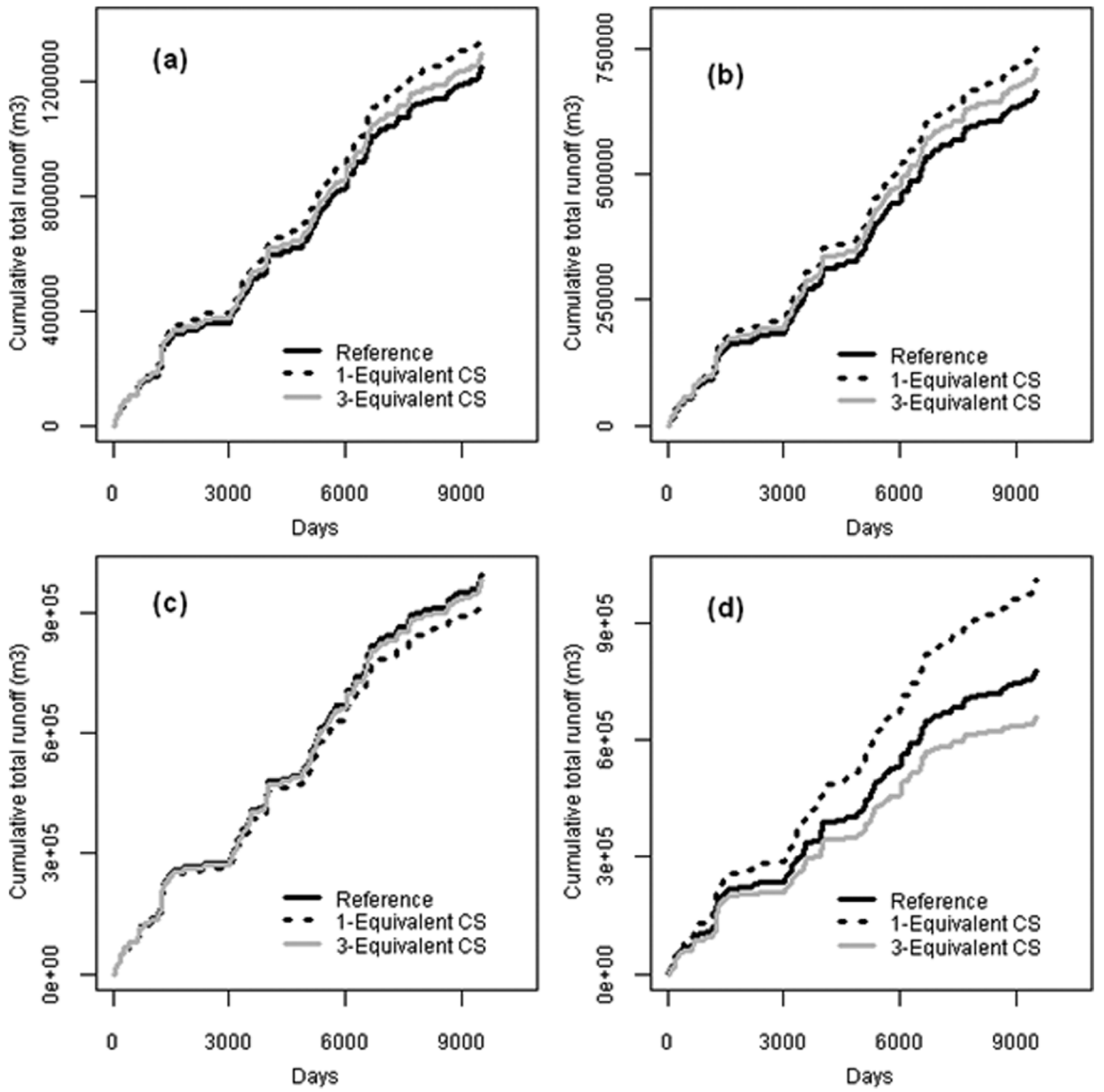

Figure 4. Cumulative total runoff for single versus three equivalent cross sections. Cumulative total runoff generated after performing the homogenization test for cross-sectional (a) length, (b) slope, (c) soil depth, and (d) soil types in subbasin M-2.

of all three equivalent cross sections are aggregated to obtain the subbasin fluxes (Figures 6a and 6b). The results of subbasin M-2 and M-7 are shown in Figures 6a and 6b indicates that the loss of accuracy is lesser than the previous two cases (Figures 4d and 5d).

4.3. Proposed Basis for Equivalent Cross-Section Formulation

The above homogenization test confirms that the amount of accuracy lost in simulated fluxes by the equivalent cross-section approach is small for averaging of length, slope, and soil depth of first-order subbasins; however, the greatest loss in accuracy occurs in the case of soil type. Therefore, careful assessment of soil-type variation is needed for formulating the equivalent cross sections. The number of equivalent cross section for a first-order subbasin is controlled by the soil-type pattern and the number of soil types. If the soil types remain unchanged within a subbasin, then a single equivalent cross section can represent the entire subbasin such as subbasin M-5 (Table 3 and Figure 2f; equation (1)–(3) applied to entire subbasin). This is so as there is little variability in soil type and soil hydraulic properties within the subbasin. If the soil types are consistent with landform pattern, i.e., different soil near the center of the river and changes toward the

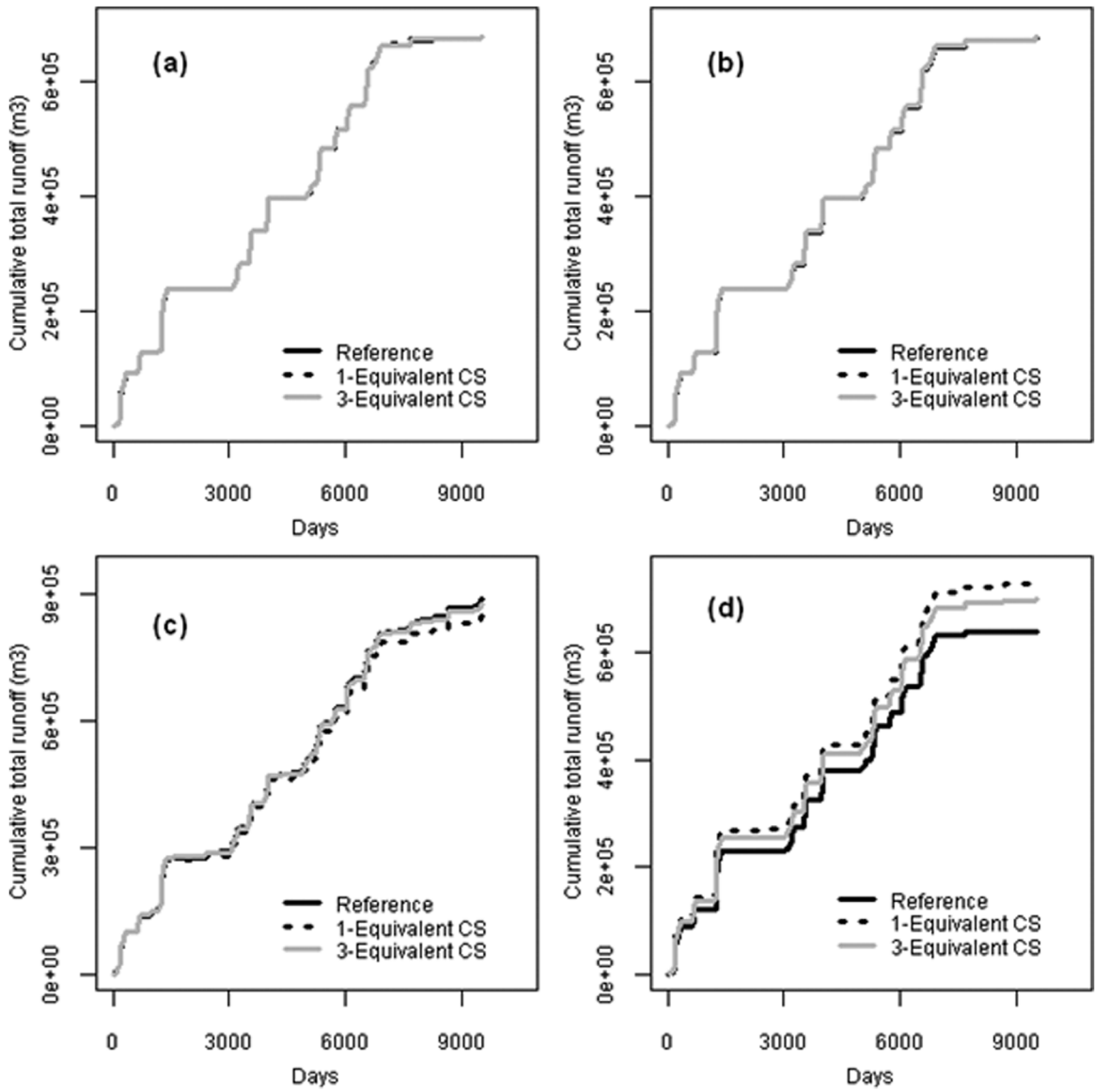

Figure 5. Cumulative total runoff for single versus three equivalent cross sections. Cumulative total runoff generated after performing the homogenization test for cross-sectional (a) length, (b) slope, (c) soil depth, and (d) soil types in subbasin M-7.

ridge line, then the three equivalent cross sections, left bank, right bank, and head water, can represent a subbasin. In this case, the variability of soil types and soil hydraulic properties is captured by the four landforms delineated as per *Khan et al*. [2013] and presented in subbasins M-1, M-3, M-6, and Wagga-Wagga (Table 3 and Figures 2b, 2d, 2g, and 2i; equations (1)–(3) and dominant soil type applied separately to each landform of equivalent cross section in left bank, right bank, and head water). If the soil types do not follow landform pattern or any other systematic pattern, at least one equivalent cross section in each soil type is required to represent a subbasin as presented in subbasins M-2, M-4, and M-7 (Table 3 and Figures 2c, 2e, and 2h; equations (1)–(3) and dominant soil type applied separately in each landform of each equivalent cross section). In this case, the variability in soil type and soil hydraulic properties of each soil polygon within the subbasin is captured by the individual equivalent cross sections.

Cumulative total runoff and cumulative transpiration using the equivalent cross-section approach are compared with the reference case for subbasin M-3, M-5, M-7, and Wagga-Wagga catchment (Figures 7a–7d and 8a–8d). The percentage difference in cumulative total runoff, transpiration, and soil evaporation between

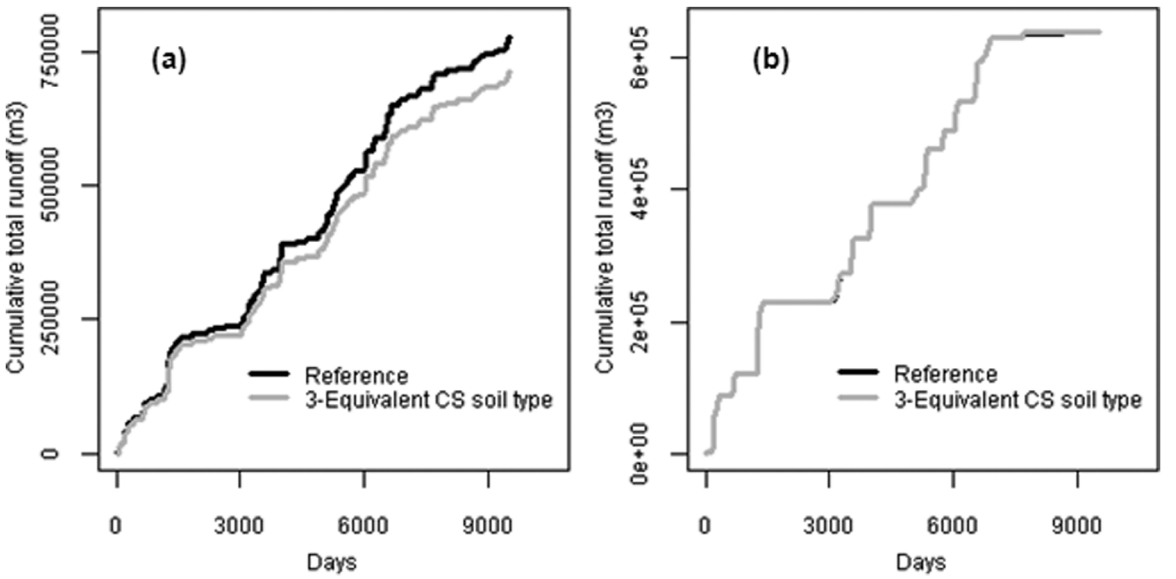

Figure 6. Formulation of three equivalent cross sections on soil-type basis for subbasin (a) M-2 and (b) M-7.

reference case and equivalent cross sections are presented in Table 4. Further, the impact of equivalent cross section on water balance is presented by calculating the fluxes in terms of percentage of rainfall (Table 5). These results show that the equivalent cross-section approach has the potential to reduce the computational time for simulating the cumulative fluxes without significant reduction in accuracy (Table 6). It should be noted that the results in Figures 7a–7d and 8a–8d represent cumulative flux plots (versus time), which illustrate the time evolution of the water balance components, included in Tables 5 and 6. Instantaneous flux plots are not included here as the focus is more on assessing whether the proposed approach is able to model overall fluxes comparably to the fully distributed case. These results are discussed further in section 5.

4.4. Validation of Equivalent Cross-Section Approach Using Observed Soil Moisture Data

To validate the equivalent cross-section approach and the soil moisture computations in U3M-2D model, the in situ soil moisture observations of Wagga-Wagga experimental catchment are used. There are total eight Neutron Moisture Metre (NMM) tubes in Wagga-Wagga experimental catchment; two are located in Tenosol, five in Chromosol, and one in Sodosol [*Tuteja et al*., 2000]. The discrete soil moisture observations are available at various depths starting from 15 cm to 1.5 m for the period of October 1997 to November 1999. Generally, soil moisture is highly heterogeneous in space; however, it is expected that the variability in soil moisture will be high if the variation in soil type, land use, topography, and climate is high, as these factors are the major drivers for generating the soil moisture and other hydrological fluxes. But, if the variation in soil type, land use, topography, and climate is low, then the spatial variability in soil moisture will be lower than the former case. The Wagga-Wagga experimental catchment is a small catchment (8.55 Ha.), where variation in land use, topography, and climate is not significant, but soil types vary significantly from the upper part of the catchment to the lower part. Therefore, simulated soil moisture was compared with soil moisture observations from individual soil types. The soil hydraulic parameters obtained from laboratory and in situ experiments are used to compare simulated and observed soil moisture (see table in the supporting information). The in situ soil moisture observations of all NMM probes located in a particular soil type and at a particular depth are compared with the simulated soil moisture of all pixels within a given landform inside the equivalent cross sections for the same soil type and soil depth (Figures 9a and 9b). Note that no averaging of soil moisture observations is performed. The in situ soil moisture observations are also compared with the reference case in a similar manner as it has been done for the equivalent cross section. For example, in Figure 9a, the in situ soil moisture observations of two NMM probes located in Tenosol at 15 cm depth (referred as "observed") are compared with the simulated soil moisture observations of all pixels in the landform-upslope of three equivalent cross sections at the same depth (referred as

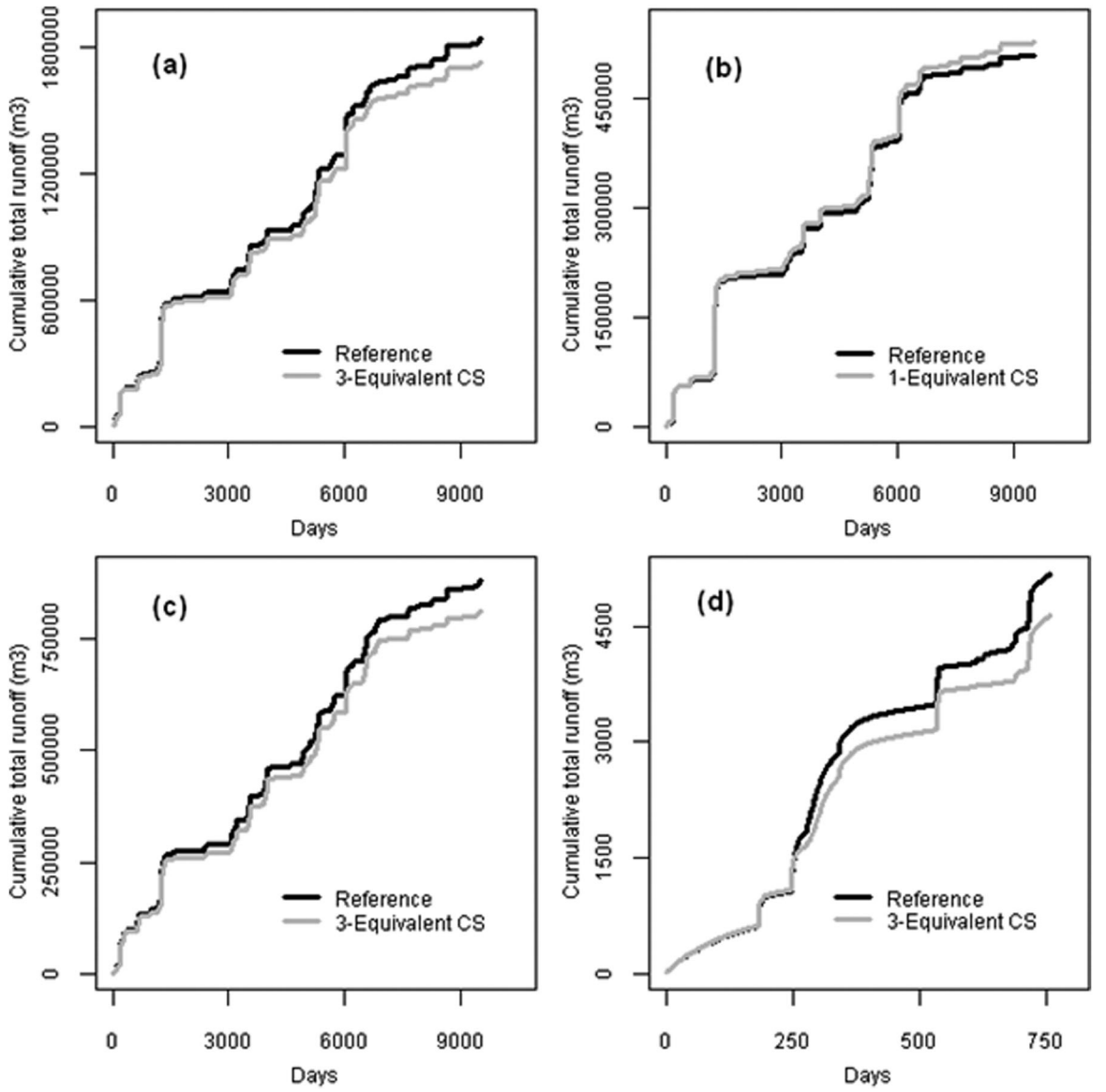

Figure 7. Comparison of cumulative total runoff for reference case and (a) three equivalent cross sections (left bank, right bank, and head water) for subbasin M-3; (b) single equivalent cross section for subbasin M-5; (c) three equivalent cross sections based on soil types for subbasin M-7; (d) three equivalent cross sections (left bank, right bank, and head water) for subbasin Wagga-Wagga.

"three equivalent cross sec"). Note that the entire Tenosol is treated as a landform-upslope in Wagga-Wagga catchment (section 2). To check the performance of U3M-2D model, the simulated soil moisture observations of all pixels in landform-upslope (Tenosol) in fully distributed hydrologic modeling (reference case) are also presented in Figure 9a (referred as "reference"). The number of points of observed soil moisture in Chromosol (Figure 9b) is higher than the Tenosol (Figure 9a) because of the higher number of NMM probes in Chromosol. The results presented in Figures 9a and 9b show that the soil moisture dynamics simulated by U3M-2D model are reasonable. The three equivalent cross sections results are also consistent with the observed soil moisture and the reference case. Further discussion about the soil moisture comparison is presented in section 5.3.

5. Discussion

The results of hydrologic modeling at multiple cross section, homogenization test, and equivalent cross section are discussed in the following subsections.

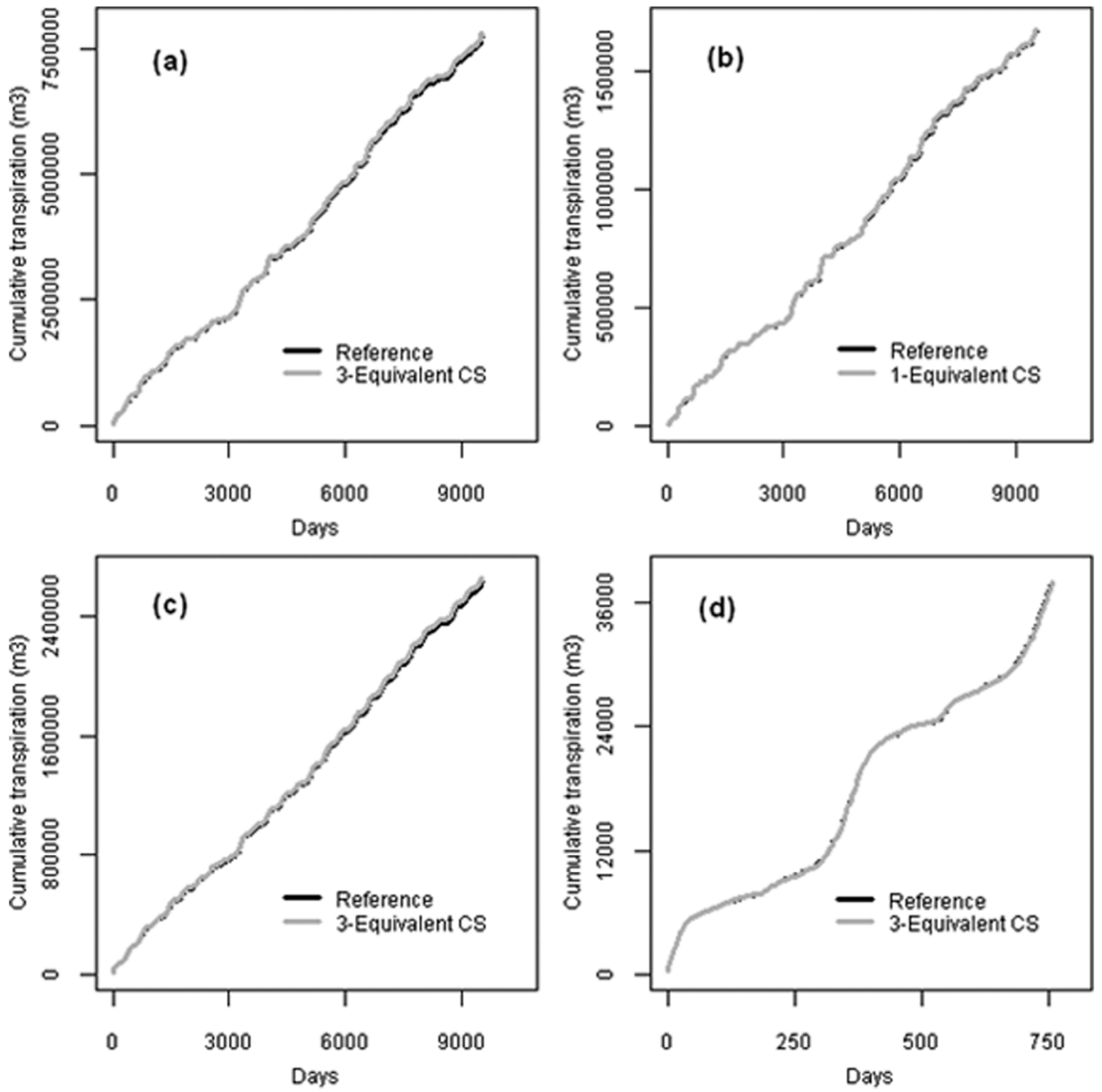

Figure 8. Comparison of cumulative transpiration for reference case and (a) three equivalent cross sections (left bank, right bank, and head water) for subbasin M-3; (b) single equivalent cross section for subbasin M-5; (c) three equivalent cross sections based on soil types for subbasin M-7; (d) three equivalent cross sections (left bank, right bank, and head water) for subbasin Wagga-Wagga.

Table 4. Comparison of Equivalent Cross-Section Results With Reference Case

Subbasin	Number of Equivalent Cross-Section	Total Runoff % Difference	Transpiration % Difference	Soil Evaporation % Difference
M-1	3	6.1	−1.8	−3.5
M-2	3	−28.1	−1.3	3.6
M-3	3	6.1	−0.9	−0.9
M-4	3	2.0	−1.9	0.0
M-5	1	−3.5	−0.1	0.4
M-6	3	7.3	−2.0	−1.0
M-7	3	7.9	−1.1	−2.3
Wagga	3	10.3	0.3	−0.8

Table 5. Total Fluxes in Terms of Percentage of Total Rainfall in Each Subbasin

Subbasin	Number of Equivalent Cross Section	Horizontal Flow (%)	Deep Drainage (%)	Transpiration (%)	Soil Evaporation (%)	Change in Storage (%)	Round Off and Weighting Error (%)
M-1	3	1.1	29.5	44.8	23.8	0.6	0.2
M-2	3	11.6	0.3	43.0	40.5	3.0	1.5
M-3	3	0.8	10.7	51.7	37.4	−1.1	0.6
M-4	3	0.7	11.8	23.6	61.4	1.7	0.8
M-5	1	2.0	5.6	23.9	67.6	0.6	0.4
M-6	3	0.5	11.1	23.8	62.2	1.4	1.1
M-7	3	0.6	15.9	53.9	29.7	−0.8	0.6
Wagga	3	1.9	2.9	39.3	59.5	−3.9	0.3

5.1. Homogenization Test

The subbasin M-2 and M-7 (Figures 2c and 2h) are used for homogenization test because of complex soil types, soil patterns, and high variability in soil hydraulic properties. Subbasin M-2 contains four types of soil: yellow earths granite, alluvial soils granite, lithosols granodiorites, and shallow red podzolics granodiorites. Subbasin M-7 contains three types of soil including shallow yellow earths granite, yellow earths granite, and earthy sands granite (Figures 2c and 2h). The saturated hydraulic conductivity of surface soil layer varies from 24 cm/d to 105 cm/d for subbasin M-2 and 38 cm/d to 105 cm/d for subbasin M-7, which is the highest amongst all subbasins (see table in the supporting information). The results of subbasin M-7 are better than those for subbasin M-2 because in subbasin M-2, the variability in cross-sectional length, contributing area, slope, and soil depth is higher than M-7 (Table 2). Furthermore, subbasin M-2 contains four types of soil whereas subbasin M-7 contains three types of soil, which also impacts the results. As shown in our analysis, the large variability in saturated hydraulic conductivities across a subbasin is successfully captured by formulating the individual equivalent cross section for each soil type. Therefore, it is expected that the equivalent cross-sections approach can be implemented in other subbasins which have single or multiple soil types and simple or complex soil pattern and are located in similar types of topographical, physiographical, and climatic conditions.

5.2. Equivalent Cross-Section Formulation

The equivalent cross-section results presented in Figures 7a–7d and 8a–8d and Table 4 show that for most of the subbasins the differences between reference case and equivalent cross-section fluxes are very low. The percentage difference between reference case and equivalent cross section in cumulative transpiration for all subbasins varies from 0.1 to 2%, whereas cumulative soil evaporation varies from 0 to 3.6%, which are significantly low (Table 4). The percentage difference between reference case and equivalent cross section in cumulative total runoff varies from 2 to 10.3% in all subbasins except subbasin M-2 (Table 4). This difference in cumulative total runoff is reasonable as the fluxes are simulated on a daily basis for 26 years of simulations. In subbasin M-2, the difference in total runoff between the reference case and equivalent cross section is 28.1% (Table 4), which is higher than other subbasins because of the complex soil pattern in this subbasin. Moreover, subbasin M-2 has the largest variability in saturated hydraulic conductivity of the surface soil layer (24–105 cm/d) compared to other subbasins impacting deep drainage and horizontal flow in particular. High variability in topographical features further impacts the differences in horizontal flows between the reference case and equivalent cross section for subbasin M-2 (Tables 2, 4, and 5). It is to be

Table 6. Reduction in Computational Time and Units Where Total Units Presents Total Number of Pixels in Each Simulation

Subbasin	Total Computational Time for Reference Case (min)	Total Computational Time for Equivalent Cross Section (min)	Ratio of Computational Time (Reference/Equivalent Cross Section)	Total Computational Units for Reference Case	Total Computational Units for Equivalent Cross Sections	Ratio of Computational Units (Reference/ Equivalent Cross Section)
M-1	175.3	28.4	6.2	232	37	6.3
M-2	151.5	21.6	7.0	218	32	6.8
M-3	129.3	19.5	6.6	285	40	7.1
M-4	307.5	47.1	6.5	270	41	6.6
M-5	84.9	3.8	22.4	251	11	22.8
M-6	358.2	52.4	6.8	265	39	6.8
M-7	197.1	26.6	7.4	319	43	7.4
Wagga	15.7	4.1	3.8	230	62	3.7

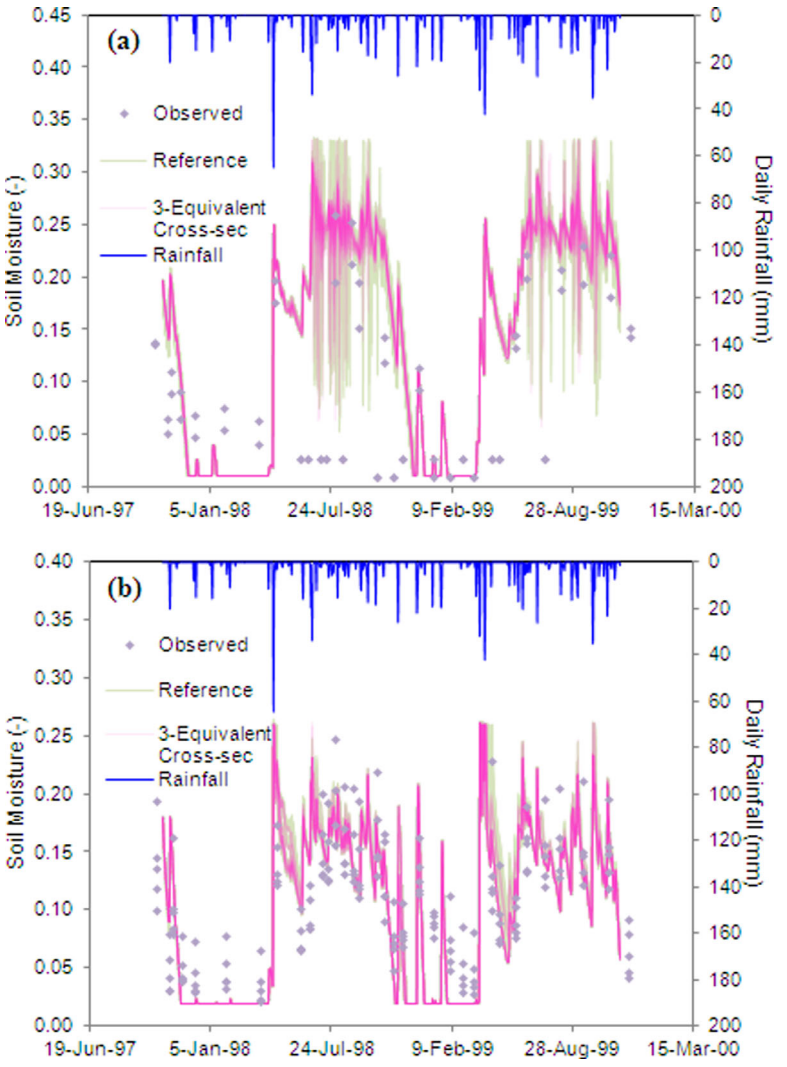

Figure 9. Comparison of observed soil moisture with simulated soil moisture for reference case and three equivalent cross sections at 15 cm depth for soil type (a) Tenosol and (b) Chromosol.

noted that the dominant fluxes in all subbasins are transpiration and soil evaporation (Table 5). The contribution of total transpiration and soil evaporation in terms of percentage of rainfall varies from 23.6 to 53.9% and 23.8 to 67.6%, respectively. These fluxes are much higher than the total horizontal flow, deep drainage, and changes in storage, which varies from 0.5 to 11.6%, 0.3 to 29.5%, and 0.6 to 3.9%, respectively (Table 5), because these catchments are dry and have significantly high evaporation demand compared to rainfall (section 2). The average horizontal flow for the seven first-order subbasins of the McLaughlin for the entire study period (1975–2000) is low (2.5% of precipitation); however, in a typical wet year (1978) horizontal flow constitutes 5.5% of precipitation, highlighting the importance of including topological connectivity in an upland catchment with a semiarid climate. The average evapotranspiration in terms of percentage of rainfall for all subbasins is around 86% whereas the average total runoff is around 14%. The fluxes which have higher contribution, transpiration, and soil evaporation are simulated with higher accuracy compared to horizontal flow and deep drainage. The amount of round off and weighting errors are negligible, i.e., 0.2–1.5% based on 26 years of simulation. These errors are introduced due to applying the different weighting/averaging techniques described in section 4 for calculating the subbasin scale fluxes. The use of equivalent cross-section approach reduces the computational time 22.4 times for subbasin M-5, in which a single equivalent cross section is formulated as it contains only one type of soil. The other subbasins in which three equivalent cross sections are formulated, the reduction of computational time varies from 3.8 to 7.4

times (Table 5). Reduction in computational time is significant for both single and three equivalent cross sections. The reduction in computational units is also of the same order.

5.3. Validation

The simulated soil moisture for both reference case and equivalent cross section are close to the observed soil moisture for Wagga-Wagga. This result confirms that the U3M-2D model captures the dynamics of soil moisture observations adequately in both soil types (Figures 9a and 9b). Only a few observations in Tenosol (Figure 9a) around 24 July 1998 are not close to the simulated values. This discrepancy is possibly caused by the macro pore flow in these conductive soils on upslopes [*McDonnell*, 1990; *McDonnell et al*., 1996; *Seibert et al*., 2003; *Weiler and McDonnell*, 2004]. Another reason for this discrepancy could be the measurement error in soil moisture observations as the chances of very low values of soil moisture records are insignificant due to the occurrence of rainfall at that time (Figure 9a). Further, such low values of observed soil moisture are not recorded in Chromosol soils at the same time which also confirms that it is most likely the measurement error (Figure 9b). Such discrepancies and mismatch between the simulated and observed soil moisture are expected as there is always a mismatch between the scale in which hydraulic conductivity and soil moisture are measured relative to the support scale of modeling elements. Furthermore, deficiencies in model structure in representing processes such as macro pore flow contribute to this problem as well. Our main goal here is to simulate dominant hydrologic processes and reduce the computational time/units in distributed hydrological modeling and the impact of scaling issues are not explicitly considered in this study.

The Wagga-Wagga experimental catchment is a dry catchment with mean annual rainfall of 534 mm/yr and mean pan evaporation of 1357 mm/yr. This catchment does not have nonzero flows. As it can been seen from the simulations, 98.8% of input rainfall is converted into evapotranspiration in this catchment and total runoff is negligible (Table 5). Considering the main role of soil moisture in water and energy balance partitioning, the evaluation of simulated soil moisture from the proposed modeling approach with the available in situ soil moisture across three types of soil and various soil depths validates the proposed approach. Needless to say, in situ soil moisture observations along with detailed topographic and physiographic information are difficult to obtain in practice. The limited soil moisture observations available for Wagga-Wagga catchment show reasonable consistency with the simulated soil moisture.

5.4. Generalization of Equivalent Cross-Section Approach

The equivalent cross-section approach for several first-order subbasins of McLaughlin catchment with various rock types and Wagga-Wagga experimental catchment is investigated here. In the equivalent cross-section formulation approach, three different categories are investigated. (1) If the soil types remain unchanged within a subbasin, then a single equivalent cross section can represent the entire subbasin. (2) If the soil types are consistent with landform pattern, i.e., different soil near the center of the river and changes toward the ridge line, then the three equivalent cross sections, left bank, right bank, and head water, can represent a subbasin. (3) If the soil types do not follow a landform pattern or any other systematic pattern, at least one equivalent cross section in each soil type is required to represent a subbasin. The extension of equivalent cross section approach for a large catchment where observed runoff is available and contains hundreds of first-order subbasins is the scope of next phase of this research. The large catchment also consists of some intermediate subbasins, which cover catchment areas located between the two junctions or stream nodes. In the case of intermediate subbasins where head water region is not available, if soil types follow a specific pattern similar to landforms (category 2), two equivalent cross sections, one on the left bank and another for the right bank, can be formulated. Further, in intermediate subbasins other two formulation categories (1 and 3) can be successfully applied as well depending on the soil-type pattern. More details on this application will be presented in a follow-up publication at a later date.

The heterogeneity in climate and land use is negligible within the first-order subbasins, used to formulate the equivalent cross section in this study. The heterogeneity in other topographical and physiographical features, i.e., length, slope, soil depth, and soil type, is well captured by the equivalent cross-section approach. The presence of four landforms in each equivalent cross section assists in capturing the variability in topographical and physiographical features. However, in catchments with highly heterogeneous soil types and complex soil pattern, the complexity can be reduced by re-grouping of soil types on the basis of similarities in soil hydraulic properties using the concept of *Murphy et al*. [2005]. This approach has been adopted in various case studies and researches in the Snowy river subbasins [*Tuteja et al*., 2006, 2007]. This

approach can be used with the equivalent cross-section approach by first re-grouping of soil types in a first-order subbasins based on hydraulic properties and then formulating the equivalent cross sections.

In this study, the equivalent cross section approach is focused on a variety of first-order subbasins in the McLaughlin catchment and Wagga-Wagga experimental catchment. The McLaughlin catchment and Wagga-Wagga experimental catchment are semiarid catchments with average annual rainfall of 650 and 534 mm/yr, respectively. In these catchments, transpiration and soil evaporation are generally the dominant fluxes impacting the total water balance, and observed runoff is either nonavailable or has zero values as in the case of the Wagga-Wagga catchment. Although transpiration and soil evaporation are simulated with reasonable accuracy using the equivalent cross-section approach, the methodology presented here is only evaluated in semiarid catchments. Future work will focus on the extension of equivalent cross-section approach in humid catchments where contribution of runoff to total water balance is larger than in the case here. Despite these limitations, development of the equivalent cross-section approach provides an effective way to reduce the computational time in distributed hydrological modeling without significant reduction in accuracy of dominant fluxes, such as transpiration and soil evaporation as examined here.

6. Conclusions

A new approach for distributed hydrological modeling using equivalent cross sections is developed in an attempt to reduce the computational time and effort in physically based distributed hydrological modeling. To formulate the equivalent cross sections, a homogenization test is carried out, which clearly indicates that soil types play a key role especially if the variability in soil hydraulic properties is significant. A single equivalent cross section is formulated for the subbasin which contains only one type of soil. Three equivalent cross sections (left bank, right bank, and head water) are formulated for the subbasins in which soil types are consistent with landform pattern, i.e., different soil type near center of the river, middle of hillslope and ridge line. Multiple equivalent cross sections are formulated for complex soil types which do not follow landform pattern or any other systematic pattern. The results of equivalent cross sections show a significant reduction in computational time/units with a slight compromise of accuracy, specifically in the fluxes that have the highest contribution in the semiarid catchments used to demonstrate the proposed logic, i.e., transpiration and soil evaporation. The accuracy achieved in total runoff simulation is also reasonable. The validation of the procedure with in situ soil moisture observations indicates that the approach and the numerical model used are capable to simulate soil moisture variability.

It can be concluded that the equivalent cross-section approach is an efficient alternative for reducing the computational requirements of distributed hydrological modeling, especially in semiarid catchments tested here, and transpiration and soil evaporation are the dominant hydrologic fluxes. The extension of equivalent cross-section approach for larger catchments, and in catchments with different climatic conditions, topography, and physiography, is the scope of future research.

Acknowledgments

This research was partly supported by the Australian Research Council, the NSW Department of Environment, Climate Change and Water (now called the NSW Office of Water), the Australian Bureau of Meteorology and the Southern Rivers Catchment Management Authority. The research benefitted greatly from discussions with David Tarboton, Lawrence Band, Garry Willgoose, and Greg Hancock during early stages of this work. We acknowledge the contributions from Brian Murphy and Brian Jenkins through extensive discussions on soils and landform issues under a variety of hydro-geomorphic settings. The DEM, climate, land use, geology, and soil data used in the study were provided to us by the former Department of Environment, Climate Change and Water, NSW.

References

Abbott, M. B., J. C. Bathurst, J. A. Cunge, P. E. O'Connell, and J. Rasmussen (1986a), An introduction to the European hydrological system—Systeme hydrologique Europeen, "SHE," 1: History and philosophy of a physically-based, distributed modelling system, *J. Hydrol.*, *87*(1–2), 45–59.

Abbott, M. B., J. C. Bathurst, J. A. Cunge, P. E. O'Connell, and J. Rasmussen (1986b), An introduction to the European hydrological system—Systeme hydrologique Europeen, "SHE," 2: Structure of a physically-based, distributed modelling system, *J. Hydrol.*, *87*(1–2), 61–77.

Argent, R. M., G. M. Podger, R. B. Grayson, K. Fowler, and N. Murray (2007), *E2 Catchment Modelling Software—User Guide*, eWater, Coop. Res. Cent. for Catchment Hydrol., Canberra, ACT., Australia.

Bathurst, J. C. (1986), Sensitivity analysis of the systeme hydrologique Europeen for an upland catchment, *J. Hydrol.*, *87*(1–2), 103–123.

Beven, K. (2001), How far can we go in distributed hydrological modelling?, *Hydrol. Earth Syst. Sci.*, *5*(1), 1–12.

Beven, K. (2006), Searching for the Holy Grail of scientific hydrology: Q(t) = H((S)under-left-arrow, (R)under-left-arrow, Delta t)A as closure, *Hydrol. Earth Syst. Sci.*, *10*(5), 609–618.

Beven, K. (2012), *Rainfall-Runoff Modelling: The Primer*, 2nd ed., Wiley-Blackwell, Chichester, U. K.

Beven, K., and A. Binley (1992), The future of distributed models: Model calibration and uncertainty prediction, *Hydrol. Processes*, *6*(3), 279–298.

Beven, K. J., and M. J. Kirkby (1979), A physically based, variable contributing area model of basin hydrology, *Hydrol. Sci. J.*, *24*(1), 43–69.

Brunner, P., and C. T. Simmons (2012), HydroGeoSphere: A fully integrated, physically based hydrological model, *Ground Water*, *50*(2), 170–176.

Downer, C. W., and F. L. Ogden (2004), GSSHA: Model to simulate diverse stream flow producing processes, *J. Hydrol. Eng.*, *9*(3), 161–174.

Flugel, W. A. (1995), Delineating hydrological response units by geographical information system analyses for regional hydrological modelling using PRMS/MMS in the drainage basin of the river Brol, Germany, *Hydrol. Processes*, *9*(3–4), 423–436.

Fortin, J., R. Turcotte, S. Massicotte, R. Moussa, J. Fitzback, and J. Villeneuve (2001a), Distributed watershed model compatible with remote sensing and GIS data. II: Application to Chaudière watershed, *J. Hydrol. Eng.*, *6*(2), 100–108.

Fortin, J., R. Turcotte, S. Massicotte, R. Moussa, J. Fitzback, and J. Villeneuve (2001b), Distributed watershed model compatible with remote sensing and GIS data. I: Description of model, *J. Hydrol. Eng.*, *6*(2), 91–99.

Grayson, R. B., I. D. Moore, and T. A. McMahon (1992a), Physically based hydrologic modeling: 2. Is the concept realistic?, *Water Resour. Res.*, *28*(10), 2659–2666.
Grayson, R. B., I. D. Moore, and T. A. McMahon (1992b), Physically based hydrologic modeling: 1. A terrain-based model for investigative purposes, *Water Resour. Res.*, *28*(10), 2639–2658.
Isbell, R. F. (1996), *The Australian Soil Classification*, 1st ed., Commonw. Sci. and Ind. Res. Organ., Collingwood, Vic., Australia.
Ivanov, V. Y., R. L. Bras, and E. R. Vivoni (2008a), Vegetation-hydrology dynamics in complex terrain of semiarid areas: 1. A mechanistic approach to modeling dynamic feedbacks, *Water Resour. Res.*, *44*, W03429, doi:10.1029/2006WR005588.
Ivanov, V. Y., R. L. Bras, and E. R. Vivoni (2008b), Vegetation-hydrology dynamics in complex terrain of semiarid areas: 2. Energy-water controls of vegetation spatiotemporal dynamics and topographic niches of favorability, *Water Resour. Res.*, *44*, W03430, doi:10.1029/2006WR005595.
Jeffrey, S. J., J. O. Carter, K. B. Moodie, and A. R. Beswick (2001), Using spatial interpolation to construct a comprehensive archive of Australian climate data, *Environ. Modell. Software*, *16*(4), 309–330.
Khan, U., N. K. Tuteja, and A. Sharma (2013), Delineating hydrologic response units in large upland catchments and its evaluation using soil moisture simulations, *Environ. Modell. Software*, *46*(2013), 142–154.
Kirchner, J. W. (2006), Getting the right answers for the right reasons: Linking measurements, analyses, and models to advance the science of hydrology, *Water Resour. Res.*, *42*, W03S04, doi:10.1029/2005WR004362.
Kollet, S. J., and R. M. Maxwell (2006), Integrated surface-groundwater flow modeling: A free-surface overland flow boundary condition in a parallel groundwater flow model, *Adv. Water Resour.*, *29*(7), 945–958.
McDonnell, J. J. (1990), A rationale for old water discharge through macropores in a steep, humid catchment, *Water Resour. Res.*, *26*(11), 2821–2832.
McDonnell, J. J., J. Freer, R. Hooper, C. Kendall, D. Burns, K. Beven, and J. Peters (1996), New method developed for studying flow on hillslopes, *Eos Trans. AGU*, *77*(47), 465–472.
McKenzie, N. J., J. C. Gallant, and L. J. Gregory (2003), Estimating water storage capacities in soil at catchment scales, *Tech. Rep. 03/3*, Coop. Res. for Catchment Hydrol., Canberra, ACT., Australia.
Minasny, B., and A. B. McBratney (2002), The neuro-m method for fitting neural network parametric pedotransfer functions, *Soil Sci. Soc. Am. J.*, *66*(2), 352–361.
Murphy, B., J. Young, J. Vaze, J. Teng, B. Jenkins, G. Summerell, and F. Townsend (2005), Soils information package to support the development of the snowy Monaro landscape plantation strategy: A report on the methodology to develop the soils information package, Dep. of Nat. Resour., Sydney, New South Wales, Australia.
Panday, S., and P. S. Huyakorn (2004), A fully coupled physically-based spatially-distributed model for evaluating surface/subsurface flow, *Adv. Water Resour.*, *27*(4), 361–382.
Paniconi, C., M. Marrocu, M. Putti, and M. Verbunt (2003), Newtonian nudging for a Richards equation-based distributed hydrological model, *Adv. Water Resour.*, *26*(2), 161–178.
Reggiani, P., and T. H. M. Rientjes (2005), Flux parameterization in the representative elementary watershed approach: Application to a natural basin, *Water Resour. Res.*, *41*, W04013, doi:10.1029/2004WR003693.
Reggiani, P., M. Sivapalan, and S. M. Hassanizadeh (1998), A unifying framework for watershed thermodynamics: Balance equations for mass, momentum, energy and entropy, and the second law of thermodynamics, *Adv. Water Resour.*, *22*(4), 367–398.
Reggiani, P., S. M. Hassanizadeh, M. Sivapalan, and W. G. Gray (1999), A unifying framework for watershed thermodynamics: Constitutive relationships, *Adv. Water Resour.*, *23*(1), 15–39.
Reggiani, P., M. Sivapalan, and S. M. Hassanizadeh (2000), Conservation equations governing hillslope responses: Exploring the physical basis of water balance, *Water Resour. Res.*, *36*(7), 1845–1863.
Schaap, M. G., and F. J. Leij (1998), Database-related accuracy and uncertainty of pedotransfer functions, *Soil Sci.*, *163*(10), 765–779.
Seibert, J., K. Bishop, A. Rodhe, and J. J. McDonnell (2003), Groundwater dynamics along a hillslope: A test of the steady state hypothesis, *Water Resour. Res.*, *39*(1), 1014, doi:10.1029/2002WR001404.
Simunek, J., M. Sejna, and M. T. van Genuchten (1999), The HYDRUS-2D software package for simulating two-dimensional movement of water, heat, and multiple solutes in variably saturated media, Int. Ground Water Model. Cent., Colo. Sch. of Mines, Golden.
Simunek, J., M. T. van Genuchten, and M. Sejna (2005), The HYDRUS-1D software package for simulating the movement of water, heat, and multiple solutes in variably saturated media, version 3.0, Univ. of Calif., Riverside.
Simunek, J., M. T. van Genuchten, and M. Sejna (2006), *The HYDRUS Software Package for Simulating Two- and Three-Dimensional Movement of Water, Heat, and Multiple Solutes in Variably-Saturated Media, Version 1.0*, PC Progress, Prague.
Singh, V. P., and D. A. Woolhiser (2002), Mathematical modeling of watershed hydrology, *J. Hydrol. Eng.*, *7*(4), 270–292.
Summerell, G. K., J. Vaze, N. K. Tuteja, R. B. Grayson, G. Beale, and T. I. Dowling (2005), Delineating the major landforms of catchments using an objective hydrological terrain analysis method, *Water Resour. Res.*, *41*, W12416, doi:10.1029/2005WR004013.
Tague, C. L., and L. E. Band (2001), Evaluating explicit and implicit routing for watersdhed hydro-ecological models of forest hydrology at the small catchment scale, *Hydrol. Processes*, *15*(8), 1415–1439.
Tague, C. L., and L. E. Band (2004), RHESSys: Regional hydro-ecologic simulation system—An object-oriented approach to spatially distributed modeling of carbon, water, and nutrient cycling, *Earth Interact.*, *8*(19), 1–42.
Tarboton, D. G. (1997), A new method for the determination of flow directions and upslope areas in grid digital elevation models, *Water Resour. Res.*, *33*(2), 309–319.
Teng, J., J. Vaze, N. K. Tuteja, and J. C. Gallant (2008), A GIS based tool for spatial and distributed hydrological modelling: CLASS spatial analyst, *Trans. GIS*, *12*, 209–225.
Tuteja, N. K., A. Rancic, J. Vaze, and G. Beale (2000), Management of key native grasses in the Murray Darling Basin, *Modell. Rep. 11/2000*, Nat. Resour. Manage. Strategy Proj., Wagga-Wagga, New South Wales, Australia.
Tuteja, N. K., J. Vaze, B. Murphy, and G. T. B. Beale (2004), CLASS: Catchment scale multiple-landuse atmosphere soil water and solute transport model, *Tech. Rep. 04/12*, Coop. Res. Cent. for Catchment Hydrol., Canberra. [Available at http://www.toolkit.net.au/Tools/CLASS-U3M-1D/publications].
Tuteja, N. K., J. Vaze, J. Teng, B. W. Murphy, and M. Mutendeudzi (2006), *Impact of Pine Plantations on Runoff From the Snowy Catchment. A Report on Outcomes From Hydrological Modelling Work to Support Landscape Strategy For the Snowy Monaro Region*, Dep. of Nat. Resour. New South Wales, Canberra.
Tuteja, N. K., J. Vaze, J. Teng, and M. Mutendeudzi (2007), Partitioning the effects of pine plantations and climate variability on runoff from a large catchment in southeastern Australia, *Water Resour. Res.*, *43*, W08415, doi:10.1029/2006WR005016.

Vaze, J., N. K. Tuteja, and J. Teng (2004), *CLASS Unsaturated Moisture Movement Model U3M-1D—User's Manual*, NSW Dep. of Infrastruct., Plann. and Nat. Resour., Sydney, Australia.

Vertessy, R. A., T. J. Hatton, P. J. O'Shaughnessy, and M. D. A. Jayasuriya (1993), Predicting water yield from a mountain ash forest catchment using a terrain analysis based catchment model, *J. Hydrol.*, *150*(2–4), 665–700.

Wagner, W., N. E. C. Verhoest, R. Ludwig, and M. Tedesco (2009), Editorial remote sensing in hydrological sciences, *Hydrol. Earth Syst. Sci.*, *13*(6), 813–817.

Watson, F. G. R., R. A. Vertessy, and R. B. Grayson (1999), Large-scale modelling of forest hydrological processes and their long-term effect on water yield, *Hydrol. Processes*, *13*(5), 689–700.

Weiler, M., and J. McDonnell (2004), Virtual experiments: A new approach for improving process conceptualization in hillslope hydrology, *J. Hydrol.*, *285*(1–4), 3–18.

Wigmosta, M. S., L. W. Vail, and D. P. Lettenmaier (1994), A distributed hydrology-vegetation model for complex terrain, *Water Resour. Res.*, *30*(6), 1665–1679.

Wood, E. F., M. Sivapalan, K. Beven, and L. Band (1988), Effects of spatial variability and scale with implications to hydrologic modeling, *J. Hydrol.*, *102*(1–4), 29–47.

Yang, D., S. Herath, and K. Musiake (1998), Development of a geomorphology based hydrological model for large catchments, *Annu. J. Eng.*, *42*, 169–174.